Supporting Information

An Integrated Microfluidic Chip for Synchronous Drug Loading, Separation and Detection of Plasma Exosomes

Yu-Xin Zhang,‡[a] Ming Wang, ‡[c] Li-Li Xu,[a] Yi-Jing Chen,[a] Shu-Ting Zhong,[a] Ying Feng,[d] Hai-Bo Zhang,*[a] Shi-Bo Cheng,*[b] Min Xie,*[a] Wei-Hua Huang[a]

[a] College of Chemistry and Molecular Sciences, Wuhan University, Wuhan 430072, P. R. China.

[b] School of Laboratory Medicine, Hubei University of Chinese Medicine, Huangjia Lake West Road, Wuhan 430065, P.R. China

[c] Department of Clinical Laboratory, Renmin Hospital of Wuhan University, Wuhan 430060. P. R China

[d] Department of Chemistry and Materials Engineering, Huizhou University, Guangdong 516007, P. R China

Table of Contents

- Table S1. Prices of partial but critical materials used for IMC.

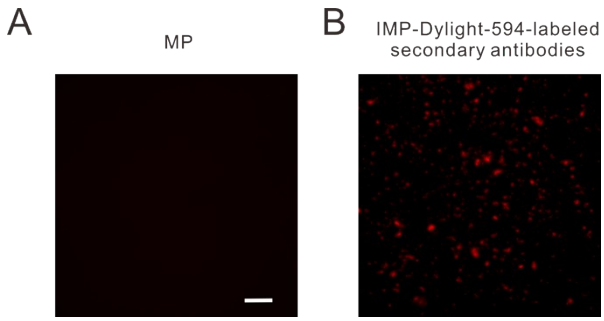

Figure S1. Fluorescent images of MP (A) and IMP (B) incubated with Dylight-594-labeled secondary antibodies, respectively. Scale bar = 50 μm.

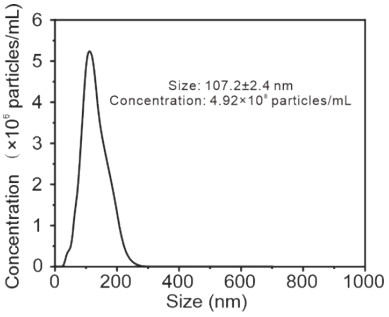

Figure S2. Particle size distribution of exosomes.

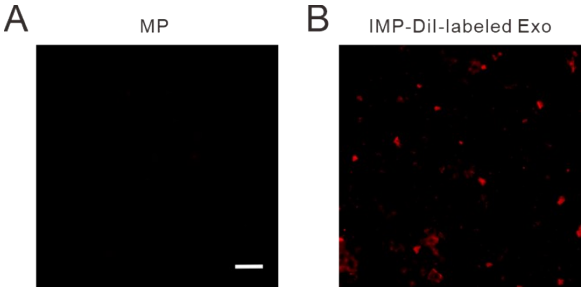

Figure S3. Fluorescent images of MP (A) and IMP (B) incubated with DiI-labeled Exo. Scale bar = 50 μm.

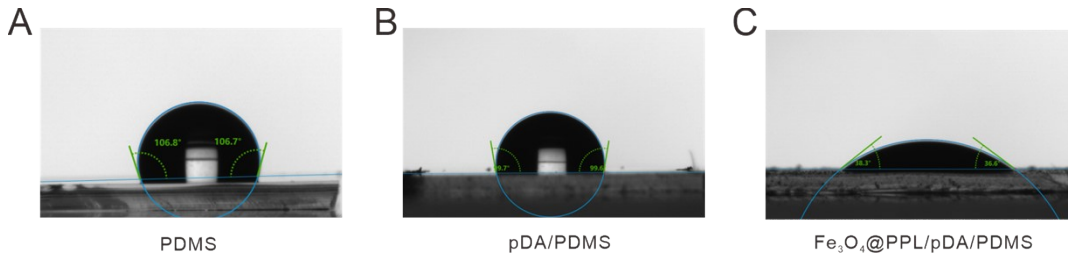

Figure S4. Contact angle measurements of PDMS film under various treatments. (A) PDMS film, (B) pDA (polydopamine)/PDMS film and (C) Fe_3O_4@PPL/pDA/PDMS film, respectively.

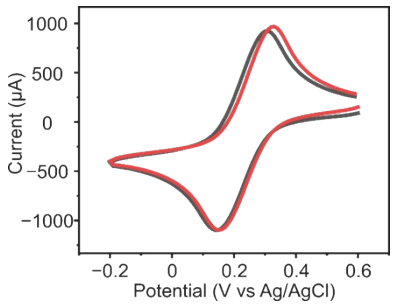

Figure S5. Cyclic voltammetry curves of magnetoresponsive electrodes from two independent fabrication batches.

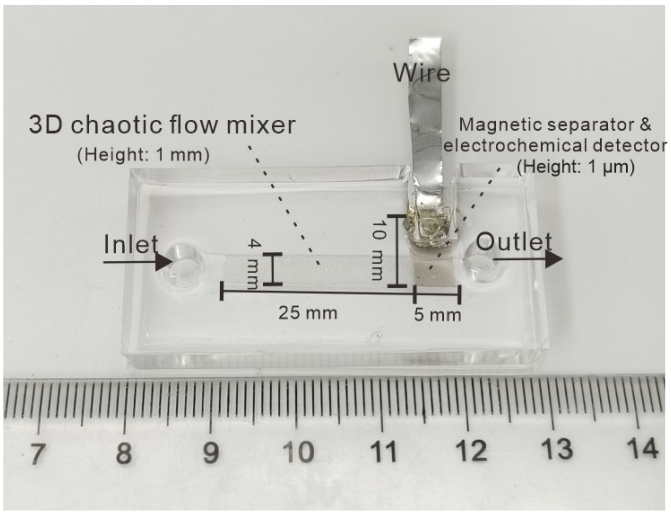

Figure S6. Photograph of the IMC.

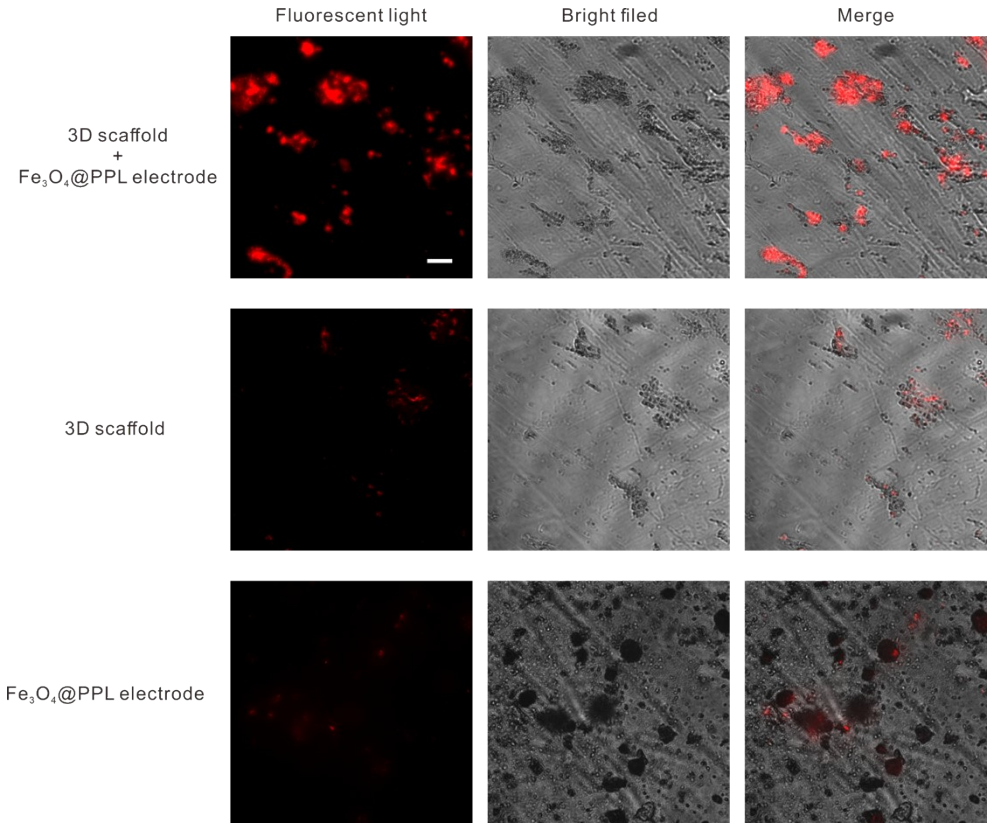

Figure S7. Fluorescent and bright filed images of the electrode in IMC under different conditions. DiI-labeled exosomes and the IMP flew through either Fe_3O_4@PPL electrode or 3D PDMS scaffold, or the IMC, respectively. Scale bar = 20 μm.

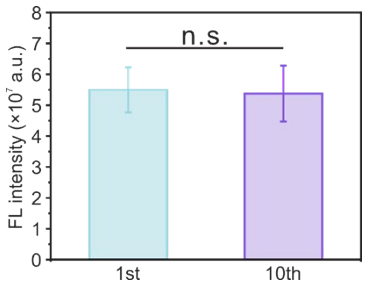

Figure S8. Fluorescence intensity of DiI-labeled exosomes captured by the magnetoresponsive electrode after the first and tenth cycles of use.

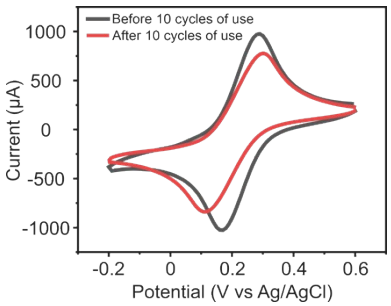

Figure S9. Cyclic voltammetry (CV) curves of the magnetoresponsive electrode before and after 10 cycles of use.

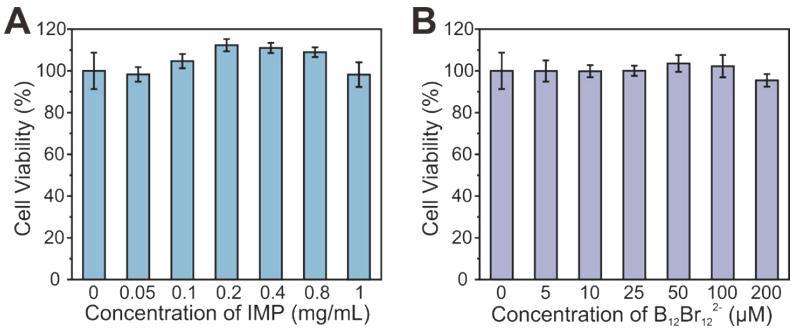

Figure S10. Cytotoxicity assay of IMP and $B_{12}Br_{12}^{2-}$. Cell viability of MCF-7/DOX cells after incubation with different concentrations of IMP (A) and $B_{12}Br_{12}^{2-}$ (B).

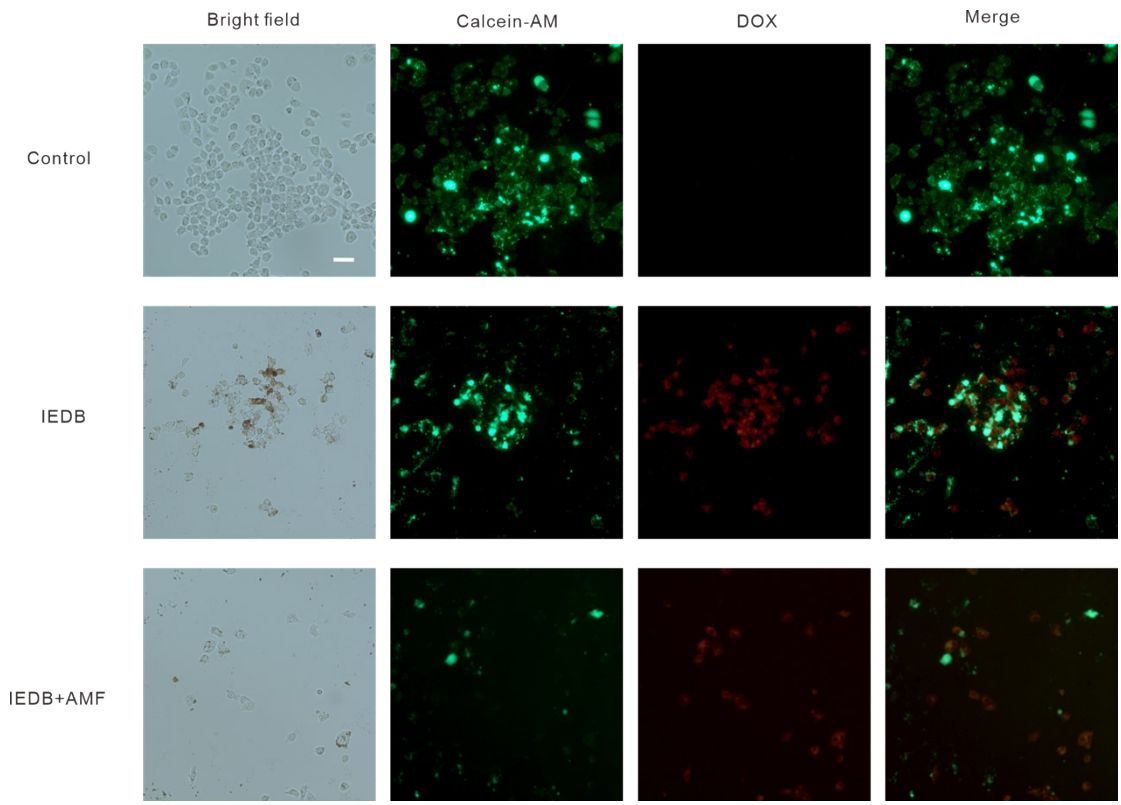

Figure S11. Fluorescent and bright filed images of MCF-7/DOX cells under different treatments. The suspended MCF-7/DOX cells were divided into three groups. One group was incubated with IEDB, another group was treated with IEDB and AMF, and the third group was used as a control. Then, they were plated on the dishes for further culture and finally stained by calcein-AM, respectively. Most of the MCF-7/DOX cells treated with IEDB (red fluorescence) or IEDB and AMF were completely damaged, so few MCF-7/DOX cells adhered to the plate and were stained by calcein-AM (green fluorescence). In contrast, the MCF-7/DOX cells without any treatment grew well and emitted bright green fluorescence of calcein-AM. Scale bar = 20 μm.

Table S1. Prices of partial but critical materials used for IMC.

Materials	Usage	Price ($)
Ni foam	33 mm × 8 mm × 1 mm	0.008
PDMS	10 g	1.580
PEDOT:PSS	4.8 μL	0.010
LiTFSI	8.16 mg	0.038
PEGylated Fe_3O_4 magnetic nanoparticles	25 μL	1.914
Sum		3.550